Characterization of OFDM Based Free Space Optical (FSO) Transmission System Under Heavy Rain Weather

Drissa Kamissoko[1], Jing He[1(✉)], Macki Tall[1], and Hassana Ganamé[2]

[1] College of Computer Science and Electronic Engineering, Hunan University, Changsha 410082, China
{idkamis2020,jhe}@hnu.edu.cn

[2] School of Electronics and Information Engineering, Huazhong University of Science and Technology, Wuhan 430074, China
hganame@hust.edu.cn

Abstract. We investigate the performance of OFDM-based FSO transmission link under heavy rain weather conditions in Ségou region, Mali. The proposed system is consisted of a single MZM modulator and a PIN photodiode that performs the optical direct detection. By selecting the convenient values for beam divergence angle and lunch power, the simulation results prove that the generated 42 Gbps OFDM data could be sent up to 1.90 km, using the Carbonneau rain attenuation Model under the worst rain conditions for the considered location.

Keywords: FSO · OFDM · Rain attenuation

1 Introduction

Nowadays, the wireless transmission links that can handle multi gigabit-per-second capacities in both back and front haul links are getting much more attention from researchers and network operators. To satisfy the increasing demand for bandwidth-hungry applications, optical communication systems are an adequate solution. The radio over fiber (RoF) system is widely utilized as a strong and low-cost solution to enhance wireless links capacity and the mobility of users [1–3]. As part of 5G mobile networks, RoF systems are sought to deliver information data from a central station (CS) to a base station (BS). Unfortunately, due to some constraints such as highways crossing or accidental regions, fiber deployment becomes expensive and impracticable. In that case, free-space optical (FSO) can be an ideal alternative to supply the equivalent capacity and quality of the fiber [4]. FSO is a wireless line-of-sight (LOS) technology that provide optical bandwidth connections through invisible light beams. Severe atmospheric attenuation such as rain can degrade the performance of the FSO link. OFDM is a high spectrally efficient modulation technique that can resist strong turbulence and achieve very high-speed transmission as the data is spread over a massive number of orthogonal

H. Jiang et al. (Eds.): ICECI 2020, LNICST 368, pp. 174–183, 2021.
https://doi.org/10.1007/978-3-030-73429-9_11

sub-carriers. OFDM-FSO system is currently being positioned as a possible 5G backhaul and fronthaul solution because it can deliver huge volumes of data at super-fast speeds, without wires.

In [2], a heterogeneous radio access network (RAN) architecture based on a hybrid RoF/FSO front hauling scenario is demonstrated to provide a resilient integration path for currently deployed 4G long term evolution (LTE) systems and the novel 5G technologies. A major drawback of FSO transmission is that bad weather conditions like fog and rain can seriously affect the FSO transmission link. Adjusting some internal parameters such as input power and beam divergence can significantly improve the transmission performance of FSO during bad weather. In [5], an FSO link was designed to transmit 20 Gbps OFDM data through 260 km in clear weather conditions. That link range was reduced to no more than 4-km due to the effects of heavy fog weather. In the paper [6], a hybrid radio over multi-mode/single-mode fiber (RoMMF/SMF)-FSO system was proposed to boost the performance of the 4G-LTE signal for the radio over indoor MMF system in the local area access networks (LAN). Similar to the optical fiber, the FSO can provide hundreds of Gigabit data rates for the broadband transmission links over short distances. In [7], a 200 Gbit/s transmission has been achieved over a 55-m outdoor FSO link by using a single 35 GHz photodiode to deliver a 32QAM dual-carrier signal; a Kramers-Kronig (KK) receiver was applied to achieve the high-capacity transmission. The performance of these systems is severely affected by the signal-signal beat interference (SSBI) caused by the square-law detection of the photodiode. In the paper [8], based on the Marshal-Palmer model and the Carbonneau model, a 16QAM-OFDM FSO communication system was proposed and investigated under heavy-rain weather in Changsha, China. During the worst rain case for a considered location that has a humid subtropical climate, a maximum bit rate of 4 Gbps could be transmitted over 6.3-km transmission distance at a bit-error-rate (BER) performance of 1.0E–3. The reference [9] investigated the impact of beam divergence using binary phase-shift keying (BPSK) and On-Off Keying (OOK) modulation schemes. The adaptive data rate method was used to reduce the BER of the proposed system. Using a narrow beam in the FSO system can generate much higher data rates and increase the link distance. Beam diverging is an indispensable phenomenon on the quality of the FSO communication system. OFDM modulation technique can mitigate the combined effect of beam diverging and atmospheric attenuation. Therefore, the effects of beam divergence on OFDM-FSO system during bad meteorological season remains an important issue to be further explored. By balancing the beam divergence and the input power adequately, the transmission range can be significantly extended without any more additional complexity.

In this paper, based on the heavy-rain weather in Ségou, Mali, a 64 QAM-OFDM baseband data is simulated to establish an FSO link to cover a distance up to 1.9 km at the data rate of 42 Gbps during the heavy rain of 79.9 mm/h. The simulation is carried out to analyze the error vector magnitude (EVM) for different beam divergence angle, the transmitting distance, and the launching power for constant rain rate and data rate. In addition, the proposed OFDM modulation format is assessed by comparing the system performance when using different rain rates as calculated based on the Carbonneau rain attenuation model.

2 Characterization of the FSO Channel Model

To design a transmission link that can resist to the atmospheric turbulence, it is of great importance to characterize the channel with proper model. We study here the impact of the beam divergence on the proposed channel model. The maximum achievable link distance is determined considering the rain attenuation model and the receive power level.

2.1 Receive Optical Power

We consider the situation of optical propagation between points in line of sight (LOS) path. Consider a single mode Gaussian beam of beam divergence angle θ and, a laser emitting a total power P_{TX}, the received power P_{RX} at an aperture of area A at range L equals [4]:

$$P_{RX} = P_{TX} * \frac{A_{RX}}{(\theta L)^2} * \tau * 10^{-\frac{\alpha L}{10}} \tag{1}$$

where α is the atmospheric attenuation coefficient along the LOS path, A_{RX} is receiver aperture size, $\tau = \tau_{TX} * \tau_{RX}$ is the combined transmitter and receiver optical efficiency. As shown in the Eq. (1), the power at the receiver is directly proportional to the transmit power and receiver aperture area, and inversely proportional to the link length and the deviation angle. Exponential part of the equation is related to atmospheric attenuation and it has the strongest influence on the link quality.

2.2 Beam Divergence Impact Analysis

Another factor that sub-serves attenuation of the signal is beam divergence. The received power can be upraised by increasing the transmitter power, the receiver area, or by diminishing the beam divergence of the transmitter beam, which is diffraction limited. The laser beam divergence is directly related to the link range as shown in (2):

$$\theta = \sqrt{\frac{P_{TX}.A_{RX}}{P_{RX}.L} * \tau * 10^{\frac{-\alpha L}{10}}} \tag{2}$$

θ can directly alter the additional noise, provoking the optical signal attenuation. The impact factor of the beam angle can be measured by taking out following term from (2) [8].

$$D_{ivg} = \frac{P_{TX}}{10^{\frac{\alpha L}{10}\theta L^2}} \tag{3}$$

In (3), we can notice that the influence of link length is more than the beam angle. A small increase in link length can introduce high additional noise. On the other hand, we can reduce the effect of increasing distance by adjusting θ, which leads us to a tradeoff between distance and beam divergence of FSO link.

2.3 Rain-Attenuation Models

Rain has pronounced impacts on electromagnetic wave propagation and one of the well-known effects is attenuation of the transmitted wave. Similarly, rain contributes to the degradation of the FSO transmission channel. In general, the rain consists of water droplets whose dimensions can vary from 100 μm to few millimeters. It is measured in attenuation per unit length [10]. The rain-attenuation is caused by geometric scattering due to raindrops. This attenuation $Att_{rain}(dB/km)$ is independent of the wavelength, but theoretically related to the raindrop size distribution, f_I, [11–16] by the following:

$$Att_{rain} = 27.29 \times 10^5 . \int_0^{\infty} r^2 . f_I dr \tag{4}$$

where:

r is the diameter of the rain drops (m).

Theoretical prediction of attenuation as a function of rainfall rate (in many cases one hour rate $R(mm/h)$) is determined using the raindrop size distribution and the International Telecommunications Union Radio communication Sector (ITU-R) recommendation [11]. For a certain location and a link distance, f_I can be given by the statistical data of rainfall rate as follows:

$$f_I = N_0 \times e^{(-8,2R^{-0,21} * r)} \tag{5}$$

with $N_0 = 8000\,\mathrm{mm}^{-1}/\mathrm{m}^3$, R is the rainfall rate in (mm/h). In practice, $0.1\,\mathrm{mm} < 2r < 5\,\mathrm{mm}$, which implies that, for the visible light and the infrared windows, the raindrop sizes are very large compared to the wavelength. This means a very large scattering cross section (effective section close to 2). The thickness of the drops, the duration of rain and the climatic zone such as tropical, temperate or equatorial climate may influence attenuation [13]. Then, the effect of Att_{rain} can be generally derived as a function of the rainfall rate using Eqs. (4) and (5).

$$Att_{rain} = \alpha * R^{\beta} \tag{6}$$

where α and β are power-law parameters. These parameters depend on the wave length, the rain drop size distribution and the rain temperature. To calculate the attenuation, it is important to make assumption that raindrops have spherical shape. This assumption makes α & β independent of polarization [15, 16]. The rain effect on the FSO link can be analyzed by knowing the rain attenuation on FSO links and corresponding rainfall intensity. Rain intensity is the fundamental parameter used to describe the rain in a given climate zone.

In this paper, the rainfall data of Ségou weather from 2012 to 2016 is studied. Ségou is the 4th administrative region of Mali, a West African country. The city is situated in the middle of the country, and it has a hot semi-arid climate. Two seasons compose the year, the rainy season (from June to September) and the dry season from October to May). Using the rainfall data reported as recorded in the climate and weather information system [18], the maximum rainfall rate within the selected period is shown in Table 1.

The Carbonneau rain-attenuation model is adopted to analyze the performance of FSO link based on the OFDM technique with 64 QAM modulation format. For this model values assigned to the parameters α and β are 1.076 and 0.67, respectively. According to the given parameters in Table 1, based on the rain Carbonneau attenuation model applied to the FSO channel, it can be seen that the rain attenuation is 21 dB/km.

Table 1. Climatic data of Ségou, Mali Latitude: 13°25′54″ longitude: 6°12′56″ latitude above sea level: 288 m

Observation period of the studied rain data	Observation date of the maximum rain intensity	Value of the maximum rain intensity observed (mm/h)	Corresponding attenuation (dB/km)
From 2012 to 2016	2016, July, 20	79.99	21

3 Simulation Setup

In the simulation, we have evaluated the system performance, considering the maximum rain attenuation level calculated from the data collected in the selected location. First, we analyze the impact of the beam divergence on the FSO link in terms of Q-factor and OSNR. Then, we have plotted the variation of the FSO link length and the EVM with respect to laser beam divergence in terms of lunch power. Finally, the constellation diagram of the received 64 QAM-OFDM formats after transmission over the FSO link considering different BD values are shown. Constant data rates of 42 Gbps is maintained during the whole simulation. The proposed OFDM–FSO system is modeled using OptiSystemTM from Optiwave Corp. As shown in Fig. 1, a 64-QAM OFDM baseband signal is used to modulate continuous wave (CW) laser using a single electrode-MZM Modulator (SD-MZM). The MZM modulator has nonlinear properties that can be exploited to eliminate the intermodulation distortion (IMD) and other nonlinear factors inherent to the modulation process [22]. A 20 dB gain optical pre-amplifier (OA) is used to boost the modulated optical signal before it is sent to the receiver through the air. In order to improve the signal strength for direct detection, an optical gain amplifier is inserted at the end of the FSO channel and before the PD.

At the receiver side, the ODD is performed using a single PIN PD. The PD delivers the electrical equivalent of the received optical signal. The low pass filter (LPF) to eliminate the unwanted signal components from the high frequency. Then, the received signal is down-converted to retrieve the original baseband data with the help of the OFDM demodulator and QAM demapper. A constellation visualizer is used to display the scatter plot of the output data. A set of parameters is given in Table 2; these parameters are optimized and used to carry the generated signal to a maximum distance. For the generation of the 42 Gbps baseband OFDM signal, the basic parameters are to be chosen according to the desired data rates [19].

Therefore, a 64 FFT block is used to map the pseudorandom- bit-sequence (PRBS) data, the central subcarrier is loaded with zero, 48 subcarriers are filled with the 64 QAM

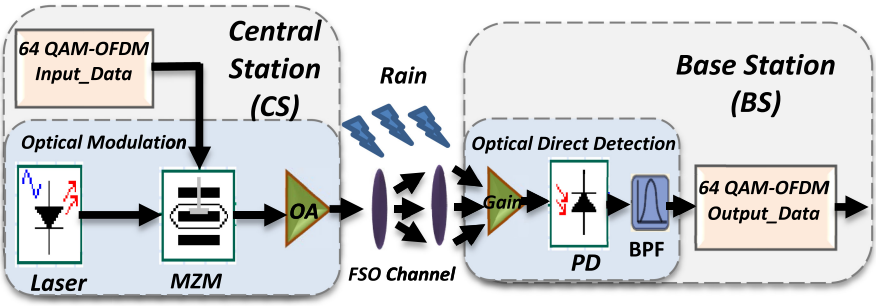

Fig. 1. Principle of FSO communication system

Table 2. System main parameters

System block	Parameters	Values
OFDM	FFT/IFFT size	64
	Number of subcarriers	52
	Data number	48
	Symbol number	80
	CP length Pilot number	16 4
FSO link	Max link range Beam divergence Transmitted power Transmitter aperture Receiver aperture	1.9 km 2–4 mrad 0–30 dBm 10 cm 30 cm
PIN photodiode	Receiver sensitivity Responsivity Dark current	20 dBm 1 A/M 10 nA

data shape, and 4 subcarriers are committed for pilot symbols. A CP of 16 samples is used to set a guard interval between OFDM symbols, and two OFDM symbols in the preamble are used for training.

A total of 502 OFDM symbols, including two OFDM training symbols, are used for the transmission simulation. Before the 64-point IFFT operation, the block of 52 QAM and 4 pilot symbols are converted into a block of 64 complex numbers such that zeros are put at positions that correspond to higher frequency subcarriers. Once this block of 64 complex numbers is ready, the last 16 complex numbers of each block are copied to the beginning of the block to constitute the CP. Then, this block of 80 complex numbers is serialized and split into I and Q components before converting to analog waveforms using digital-to-analog converters (DACs). A symbol-rate/subcarrier of 146 Mbaud is chosen in our system that results in a useful bit rate of 42 Gbps using 64-QAM ($48 \times 146 \times 6$).

4 Simulation Results

Figure 2a) shows the Q-factor degradation with the increasing BD. It can be noticed that increasing the BD angle deteriorates the link performance. The Q-factor decreases progressively and worsens the link quality. In order to display the OSNR variation and evaluate the maximum achievable link distance under the worst rain weather conditions in the considered location, we have chosen two different values of beam divergence that are 2 mrad and 4 mrad. In practice, minimizing the divergence angle implies accurate alignment between the transmitter and the receiver. In the case of the mobility of the receiver, to improve the received power and ease the alignment between the communicating terminals, an adaptive beam technique is generally implemented [23]. It consists of adapting the divergence angle according to the receiver aperture diameter and the communication distance. In Fig. 2b), we explain the change in the Q-factor vs. optical signal to noise ratio (OSNR) characteristic considering BD values of 2mrad and 4mrad. We assess the performance of the proposed system by adding a certain amount of noise using the Set OSNR block of Optisystem software; then, we measure the corresponding received Q-factor values. It can be noted that a global increase of the OSNR from 5 dB to 60 dB improves the Q value from 15.52 dB to 17.01 dB. It means that a great variation in OSNR has only a slight influence on the Q-factor. The obtained graphs prove that the link can tolerate more attenuation by decreasing the divergence angle. The maximum achievable link distance for 2 mrad and 4 mrad beam divergence is displayed in Fig. 3a). In Fig. 3b), the FSO range and the EVM level are evaluated, varying the input power. At 0 dBm lunch power, a range of 0.8 km with receive power of −14.760 dBm was achieved for 2 mrad; and 0.63 km, −14.947 dBm link range and optical power were achieved for 4 mrad. Upgrading the lunch power to 30 dBm, the link range linearly increases up to 1.90 km for −15.108 dBm received and 1.60 km for −14.557 dBm respectively for 2 mrad and 4 mrad divergence angles. Observing the EVM variation in Fig. 3b), albeit the significant deterioration of the EVM with the increasing power, 30 dBm lunch power can be supported in our proposed system for both selected angle values. It can be observed that after 1.9 km in the heavy and 2 mrad divergence angle, the EVM is less than 8%. It proves that the 64 QAM-OFDM formats are less affected in the FSO channel regardless of the raindrop size. The EVM is 7.8% and the performance is less when transmitting 42 Gbps data rate within an FSO channel using a beam divergence of 4 mrad.

Figure 4 shows the constellation of the 64 QAM-OFDM formats after different transmission distances over the FSO channel. From Fig. 4a), the clear constellation of the received signal after 1.90 km with 2 mrad divergence angle can be seen. The receive constellation after 1.60 km with 4 mrad is less clear and acceptable, as shown in Fig. 4b).

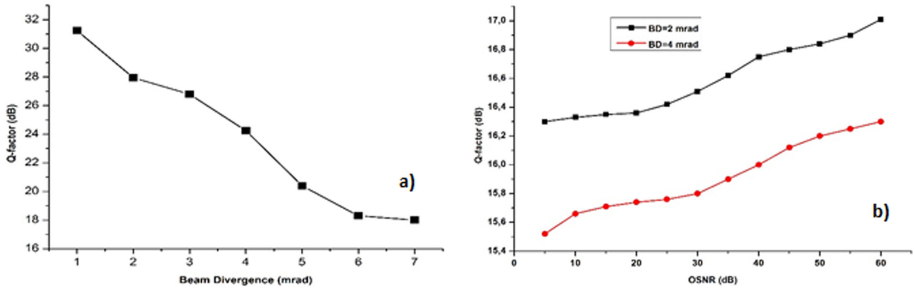

a) Q-factor vs. Beam Divergence b) Q-factor vs. OSNR

Fig. 2. a) Q-factor vs. Beam Divergence b) Q-factor vs. OSNR

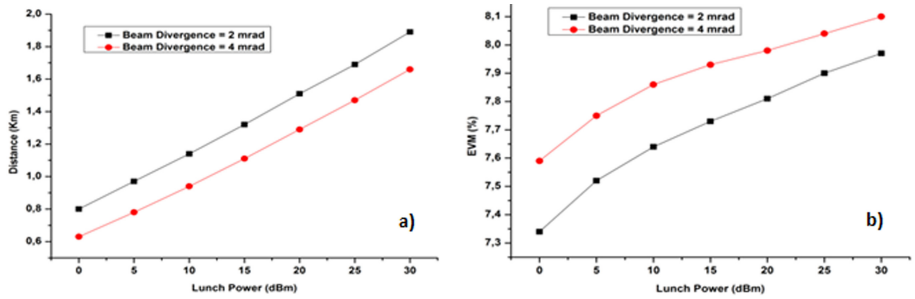

Fig. 3. a) the maximum achievable distance depending on the lunch power b) the EVM values depending on the lunch power.

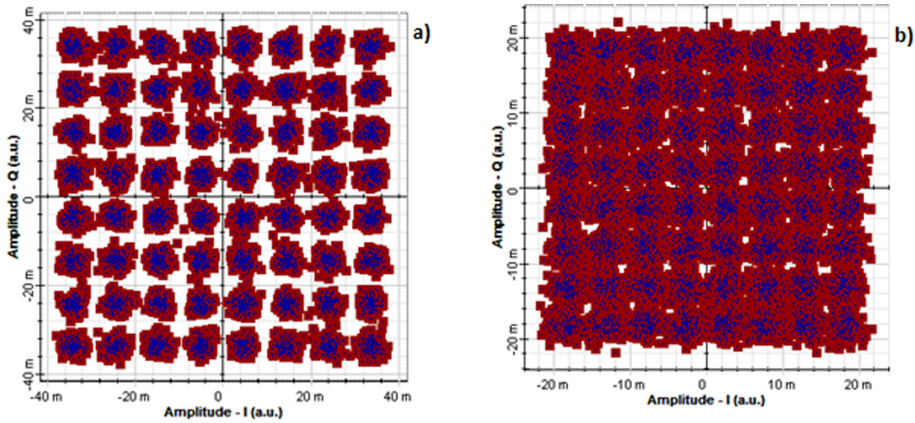

Fig. 4. The constellation of 64 QAM-OFDM format after transmission over FSO link a) with beam divergence angle of 2 mrad, b) with beam divergence angle of 4 mrad.

5 Conclusion

In the paper, we have investigated a 64 QAM-OFDM FSO transmission system under heavy-rain weather in Ségou, Mali. The performance of the OFDM-FSO system based on the Carbonneau Model was assessed. The effect of beam divergence was also analyzed, and results revealed that the quality of the reception decreases on the high broadening of the FSO transmitter light beam. It is evident that raising the transmit power augment the performance and make the system able to achieve prolonged transmission distance. Up to 1.90 km is reached for the same performance.

References

1. Chang, G., Peng, P.: Grand challenges of fiber wireless convergence for 5G mobile data communications. In: 2018 23rd Opto-Electronics and Communications Conference (OECC), Jeju Island, Korea (South), pp. 1–2 (2018)
2. Mufutau, A.O., Guiomar, F.P., Fernandes, M.A., Lorences-Riesgo, A., Oliveira, A., Monteiro, P.P.: Demonstration of a hybrid optical fiber–wireless 5G fronthaul coexisting with end-to-end 4G networks. IEEE/OSA J. Opt. Commun. Netw. **12**(3), 72–78 (2020)
3. Dat, P.T., Kanno, A., Kawanishi, T.: Low-latency fiber-wireless bridge for flexible fronthauling in future mobile networks. In: 2015 10th European Microwave Integrated Circuits Conference (EuMIC), Paris, pp. 305–308 (2015)
4. Pham, A.T., Trinh, P.V., Mai, V.V., Dang, N.T., Truong, C.T.: Hybrid free-space optics/millimeter-wave architecture for 5G cellular backhaul networks. In: 2015 Opto-Electronics and Communications Conference (OECC), Shanghai, pp. 1–3 (2015)
5. Singh, R., Soni, G.: Realization of OFDM based free space optics. In: 2015 International Conference on Green Computing and Internet of Things (ICGCIoT), Noida, pp. 32–35 (2015)
6. Al-Musawi, H.K., et al.: Fundamental investigation of extending 4G-LTE signal over MMF/SMF-FSO under controlled turbulence conditions. In: 2016 10th International Symposium on Communication Systems, Networks and Digital Signal Processing (CSNDSP), Prague, pp. 1–6 (2016)
7. Lorences-Riesgo, A., Guiomar, F.P., Sousa, A.N., Teixeira, A.N., Muga, N.J., Monteiro, P.P.: 200 Gbit/s free-space optics transmission using a Kramers-Kronig receiver. In: 2019 Optical Fiber Communications Conference and Exhibition (OFC), San Diego, CA, USA, pp. 1–3 (2019)
8. Rashidi, F., et al.: Performance investigation of FSO–OFDM communication systems under the heavy rain weather. J. Opt. Commun. **39**, 37–42 (2016)
9. Awan, M.B., Mohan, S.: Analysis of beam divergence and input bit rate for free space optical communication link. In: 2016 IEEE 37th Sarnoff Symposium, Newark, NJ, pp. 83–87 (2016)
10. Grover, A., Sheetal, A.: Improved performance investigation of 10 Gb/s–10 GHz 4-QAM based OFDM-Ro-FSO transmission link. J. Opt. Commun. eISSN 2191–6322, ISSN 0173-4911
11. Report ITU-R F.2106–1 (11/2010), Fixed service applications using free-space optical links. https://www.itu.int/pub/R-REP-F.2106-2007
12. Norouzian, F., et al.: Rain attenuation at millimeter wave and low-THz frequencies. IEEE Trans. Antennas Propag. **68**(1), 421–431 (2020). https://doi.org/10.1109/TAP.2019.2938735
13. Dath, C.A.B., Faye, N.A.B.: Resilience of long range free space optical link under a tropical weather effects. Sci. Afr. **7**, e00243 (2020). www.elsevier.com/locate/sciaf. Accessed 13 Nov 2019

14. Benestad, R.E., Parding, K.M., Erlandsen, H.B., Mezghani, A.: A simple equation to study changes in rainfall statistics. Environ. Res. Lett. **14**, (2019)
15. Shrestha, S., Choi, D.Y.: Characterization of rain specific attenuation and frequency scaling method for satellite communication in South Korea. Int. J. Antennas Propag, Article ID 8694748, 16 (2017)
16. Shrestha, Sujan, Choi, Dong-You: Rain attenuation statistics over millimeter wave bands in South Korea. J. Atmos. Solar-Terrestrial Phys. Volumes **152–153**, 1–10 (2017)
17. Adirosi, E., Volpi, E., Lombardo, F., Baldini, L.: Raindrop size distribution: fitting performance of common theoretical models. Adv. Water Res. **96**, 290–305 (2016)
18. Agence Nationale de la Météorologie (MALI-METEO) Copyright © 2020. Sise Zone Aéroportuaire de Bamako-Sénou | BP: 237 Tél. (223) 20 20 62 04 - Fax: 223) 20 20 21 10 site web: http://www.malimeteo.ml/
19. Li, C.X., Shao, Y.F., Wang, Z.F., Zhou, J.Y., Zhou, Y., Ma, W.Z.: Optical 64QAM-OFDM transmission systems with different sub-carriers. Opt. Photonics J. **6**, 196–200 (2016)
20. Liu, X., et al.: 128 Gbit/s free-space laser transmission performance in a simulated atmosphere channel with adjusted turbulence. IEEE Photonics J. **10**(2), 1–10 (2018)
21. Chen, H., Chi, Y., Lin, C., Lin, G.: Adjacent channel beating with recombined dual-mode colorless FPLD for MMW-PON. IEEE J. Sel. Topics Quantum Electron. **23**(6), 1–9 (2017)
22. Sun, J., Yu, L., Zhong, Y.: A single sideband radio-over-fiber system with improved dynamic range incorporating a dual-electrode dual-parallel Mach-Zehnder modulator. Opt. Commun. **336**(1), 315–318 (2015)
23. Kaymak, Y., et al.: Beam with adaptive divergence angle in free-space optical communications for high-speed trains. http://arxiv.org/arXiv:1812.11233, 28 December 2018